



Original Research Article

Graphene Oxide@Polyaniline-FeF₃ (GO@PANI-FeF₃) as a Novel and Effectual Catalyst for the Construction of 4*H*-Pyrimido [2, 1-*b*] Benzothiazoles

Mohammad Kamali-Ardakani , Esmael Rostami* , Abdolkarim Zare

Department of Chemistry, Payame Noor University, PO Box 19395-4697, Tehran, Iran

ARTICLE INFO

Article history

Submitted: 04 November 2023

Revised: 25 December 2023

Accepted: 31 December 2023

Available online: 13 January 2024

Manuscript ID: [AJCA-2312-1460](https://doi.org/10.48309/ajca.2024.428749.1460)

Checked for Plagiarism: **Yes**

Language editor:

[Dr. Fatimah Ramezani](#)

Editor who approved publication:

[Dr. Sami Sajjadifar](#)

DOI: [10.48309/ajca.2024.428749.1460](https://doi.org/10.48309/ajca.2024.428749.1460)

KEYWORDS

Nanocomposite

Graphene oxide@polyaniline-FeF₃
(GO@PANI-FeF₃)

4*H*-Pyrimido[2,1-*b*]benzothiazole

2-Aminobenzothiazole

ABSTRACT

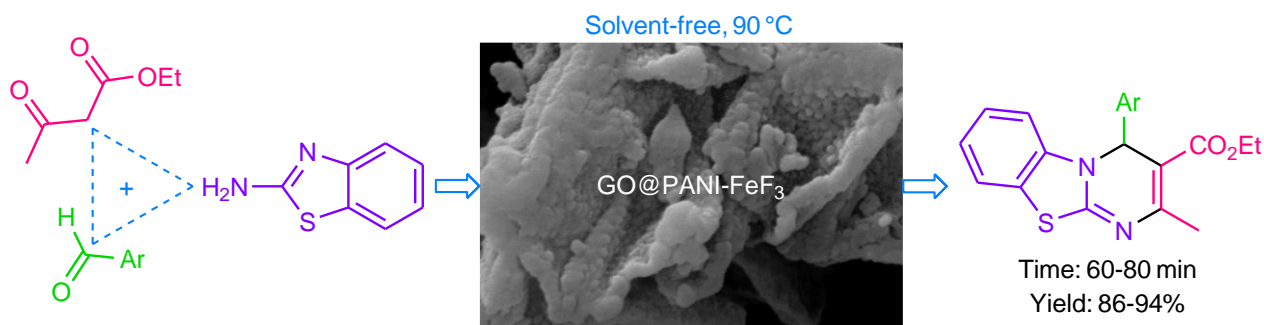
A thermally and chemically sustainable nanocomposite, namely graphene oxide@polyaniline-FeF₃ (GO@PANI-FeF₃), was fabricated, and characterized using FT-IR (Fourier transform infrared spectroscopy), XRD (X-ray diffraction), FE-SEM (field emission scanning electron microscopy), EDAX (energy-dispersive X-ray spectroscopy), and TG (thermal gravimetric) analyses, and then 4*H*-pyrimido[2,1-*b*]benzothiazoles were constructed from aryl aldehydes, ethyl acetoacetate, and 2-aminobenzothiazole using GO@PANI-FeF₃ as catalyst; performing the reactions under solvent-free conditions, efficiency, high yields, relatively short times, and recoverability of the catalyst are some advantages of our protocol.

* Corresponding author: Rostami, Esmael

✉ E-mail: e.rostami@pnu.ac.ir

© 2024 by SPC (Sami Publishing Company)

GRAPHICAL ABSTRACT



Introduction

Because of our closed ecosystem, sustainable catalysts are of great importance for future of chemistry. During chemical transformations, diverse wastes are produced and accumulated in the environment. To avoid the risks, sustainable catalysts and reagents help us to preserve the environment. Reusing catalysts and wastes in the consecutive cycles is an important approach to solve environmental crises and economical aspects [1]. Nanostructured materials are superior in comparison with bulk ones [2-12]. For example, nanocatalysts are applied in fewer amounts, and mostly are reusable; thus, they are good candidates for sustainable processes, and are helpful to perform chemical reactions in safe medium [5-12]. Graphene and graphene oxide based nanomaterials are an attractive and valuable category of nanocatalysts, which have been utilized to carry out a variety of organic transformations [8-12]. Production of materials for daily life should be done without harming the environment. For this purpose, chemical processes should be designed in accordance with green chemistry principals [13]. A useful way to diminish the environmental problems is utilization of one-pot multi-component reactions (MCRs) in organic synthesis. In MCRs, formation of by-products and wastes, energy consumption and the use of toxic organic solvents are minimized, time and economy is saved, and

product yield is increased [14-18]. The substances bearing benzothiazole scaffold are a significant class of heterocycles, because they have numerous biological and medicinal activities, e.g., antitumor [19], antimicrobial [20], antioxidant [21], antidiabetic [22], anti-infective [23], anticonvulsant [24], antibacterial [25], and anti-tubercular [26] properties. The one-pot multi-component reaction of aryl aldehydes, ethyl acetoacetate and 2-aminobenzothiazole is a useful method to construct 4*H*-pyrimido[2,1-*b*]benzothiazoles; some catalysts have been utilized to perform this reaction, e.g., trypsin [27], acetic acid-activated charcoal [28], Fe₃O₄@nano-cellulose/TiCl₄ [29], carbon/TiO₂-SO₃H-SbCl₅ [30], nano-cellulose/BF₃/Fe₃O₄ [31], Fe₃O₄@nano-dextrin-OPO₃H₂ [32], nano-kaolin/Ti⁴⁺/Fe₃O₄ [33], 1,1,3,3-tetramethylguanidinium trifluoroacetate [34], and [NiTC]HSO₄@Fe₃O₄ [35]. Many of the reported methods for the construction of 4*H*-pyrimido[2,1-*b*]benzothiazoles have one or more of these drawbacks: moderate yields, long reaction times, difficult purification, high temperature, and no reusability of catalyst.

Concerning the above issues, introducing a novel graphene oxide-based nanocomposite to catalyze the multi-component reaction of aryl aldehydes, ethyl acetoacetate and 2-aminobenzothiazole in solvent-free conditions leading to 4*H*-pyrimido[2,1-*b*]benzothiazoles is valuable and desirable. Here, we have exactly

done this, and introduced graphene oxide@polyaniline-FeF₃ (GO@PANI-FeF₃) nanocomposite as an effectual catalyst for the construction of 4*H*-pyrimido[2,1-*b*]benzothiazoles.

Experimental

Materials

Chemicals and solvents (in high purity) were purchased from Sigma-Aldrich chemical company, and utilized without further purification. The modified Hummers method was utilized to construct graphene oxide (GO) [36]. For recording NMR spectra, Bruker Avance device was employed. JASCO FT-IR spectrometer was utilized to record FT-IR spectra using KBr pellets. A Shimadzu apparatus (XRD 6000) was exploited for recording XRD patterns. FE-SEM and EDAX were recorded using a TESCAN electron microscope. TGA was studied using a Perkin Elmer (Elan DRC 6000) device.

Fabrication of GO@PANI

GO (0.20 g) was added to HCl solution (1M, 70 mL), and the mixture was sonicated for 60 min at room temperature. The attained suspension was cooled in an ice bath for 30 min, aniline (40 mmol, 3.66 mL) was added, and vigorously stirred. Separately, a solution of (NH₄)₂S₂O₈ (40 mmol, 9.1 g) in HCl (1 M, 30 mL) was prepared, and cooled in an ice bath for 30 min, and then it was added to the GO-aniline mixture, and the resulting mixture was stirred in ice bath for 10 h. Finally, the formed precipitate was filtered, washed with deionized water, and dried in a vacuum oven at 60 °C to afford GO@PANI. Polymerization of aniline was performed according to the literature [37].

Fabrication of GO@PANI-FeF₃

A solution of GO@PANI (0.50 g) in acetonitrile (25 mL) was sonicated at room temperature for 1 h, and then FeF₃ (1 mmol, 0.113 g) was added to it, and the obtained mixture was stirred at 60 °C for 24 h. Lastly, the precipitate was filtered, washed with acetic acid, acetonitrile and acetone, and dried in an oven at 100 °C to obtain GO@PANI-FeF₃.

The construction of 4*H*-pyrimido[2,1-*b*]benzothiazoles

A mixture of aldehyde (1 mmol), ethyl acetoacetate (1 mmol, 0.13 g), 2-aminobenzothiazole (1 mmol, 0.15 g) and GO@PANI-FeF₃ (0.02 g) was homogenized by a glass rod, and stirred at 90 °C. After the completion of the reaction (as monitored by TLC using silica gel SIL G/UV 254), hot EtOAc was added, stirred, and filtered hot to isolate insoluble GO@PANI-FeF₃ (which was washed by hot EtOAc and dried). The filtrate was distilled, and the retained solid was recrystallized from EtOH to give pure 4*H*-pyrimido[2,1-*b*]benzothiazole.

NMR data of 4*H*-Pyrimido[2,1-*b*]benzothiazole **4d**

¹H-NMR (400 MHz, DMSO-*d*₆): δ (ppm) 1.21 (t, *J* = 7.1 Hz, 3H, CH₃CH₂), 2.51 (s, 3H, CH₃), 4.07 (m, 2H, CH₂CH₃), 6.66 (s, 1H, methine CH), 7.21 (t, *J* = 7.6 Hz, 1H, Ar), 7.31 (t, *J* = 7.7 Hz, 1H, Ar), 7.47 (d, *J* = 8.1 Hz, 1H, Ar), 7.73-7.78 (m, 3H, Ar), and 8.16 (d, *J* = 8.2 Hz, 2H, Ar); ¹³C-NMR (100 MHz, DMSO-*d*₆): δ (ppm) 14.6, 23.9, 56.4, 60.2, 102.3, 112.8, 123.3, 123.5, 124.4, 124.8, 127.4, 128.9, 137.7, 147.7, 148.7, 155.5, 163.5, and 165.7.

Results and Discussion

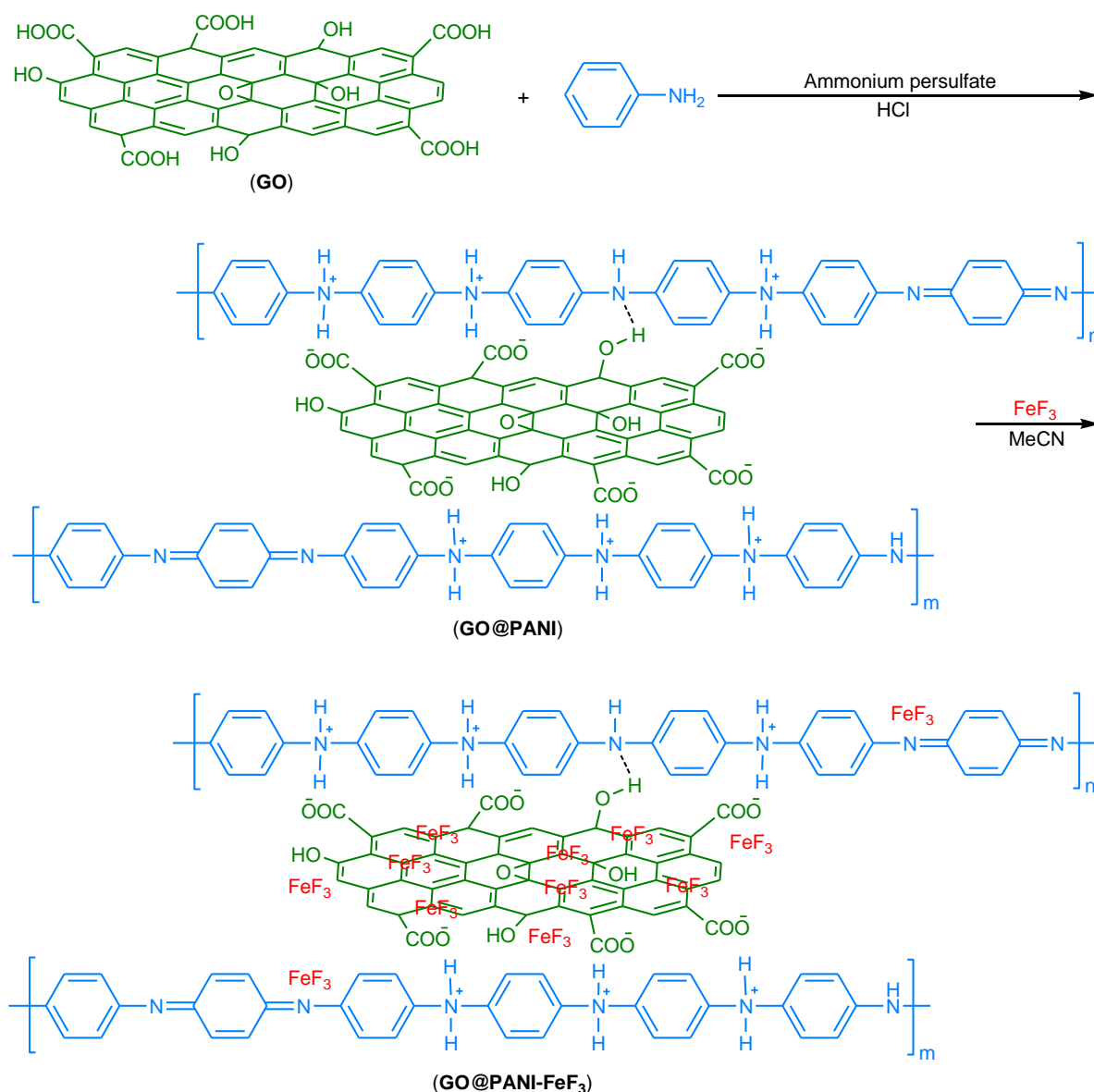
Characterization of GO@PANI-FeF₃

Graphene oxide@polyaniline-FeF₃ (GO@PANI-FeF₃) was fabricated according to Scheme 1; FT-IR, EDAX, FE-SEM, XRD, and TG analyses were

applied for its characterization. In the FT-IR spectrum of GO (Figure 1), the peak related to hydroxyl groups was observed at 3410 cm^{-1} . Carbonyl groups gave a peak at 1739 cm^{-1} [38]. The band appeared at 1628 cm^{-1} is related to C=C bonds [39]. The peak corresponded to epoxide C-O was observed at 1053 cm^{-1} [40]. In the FT-IR spectrum of GO@PANI (Figure 2), the band at 3391 cm^{-1} is ascribed to NH of polyaniline, and the broad peak appeared at $\sim 3100\text{-}3650\text{ cm}^{-1}$ is related to hydroxyl groups of GO [41]. The bands observed at ~ 3031 and $\sim 2918\text{ cm}^{-1}$ are belong to aromatic and aliphatic C-H bonds, respectively

[42]. C=C groups gave bands at 1593 and 1497 cm^{-1} . The peak appeared at 1296 cm^{-1} can be attributed to C-N bonds of polyaniline [43]. The peak belong to C-O was observed at 1107 cm^{-1} [44]. In the FT-IR spectrum of GO@PANI-FeF₃ (Figure 3), the bands related to NH and hydroxyl groups were detected at 3445 and 3252 cm^{-1} , respectively [41].

The peak at 1674 cm^{-1} is ascribed to C=O groups. C=C bonds gave peaks at 1582 and 1493 cm^{-1} . The peak belong to C-N was seen at 1300 cm^{-1} [43]. The peak related to Fe-F bonds of FeF₃ was observed at 501 cm^{-1} [45].



Scheme 1. Fabrication of GO@PANI-FeF₃.

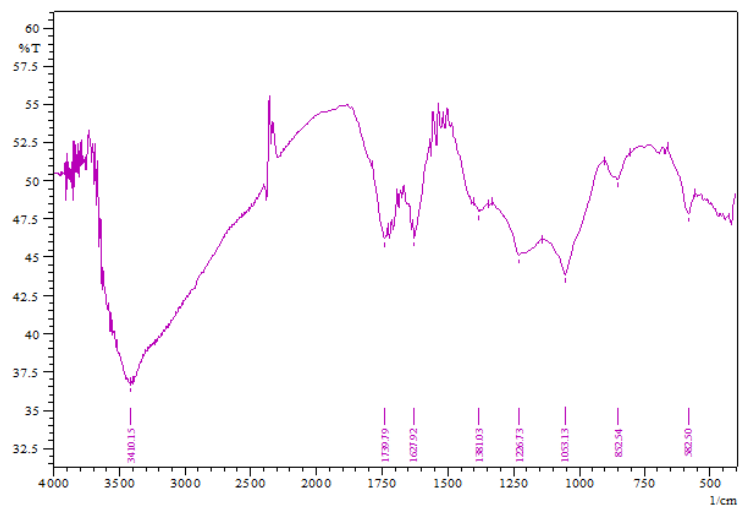


Figure 1. The FT-IR spectrum of GO.

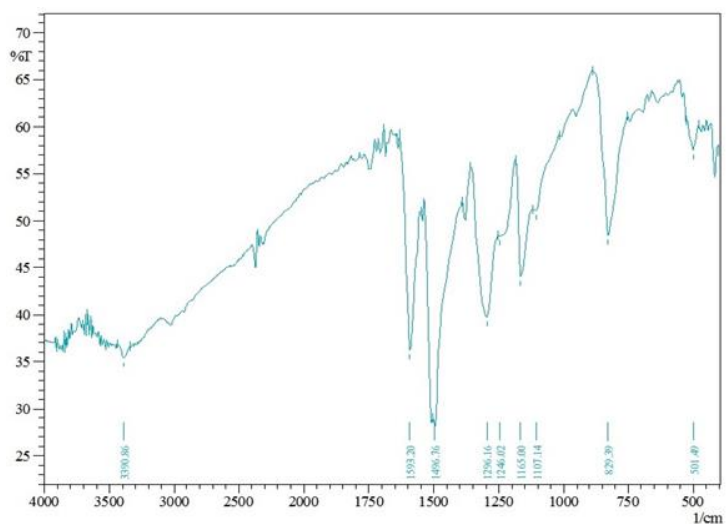


Figure 2. The FT-IR spectrum of GO@PANI.

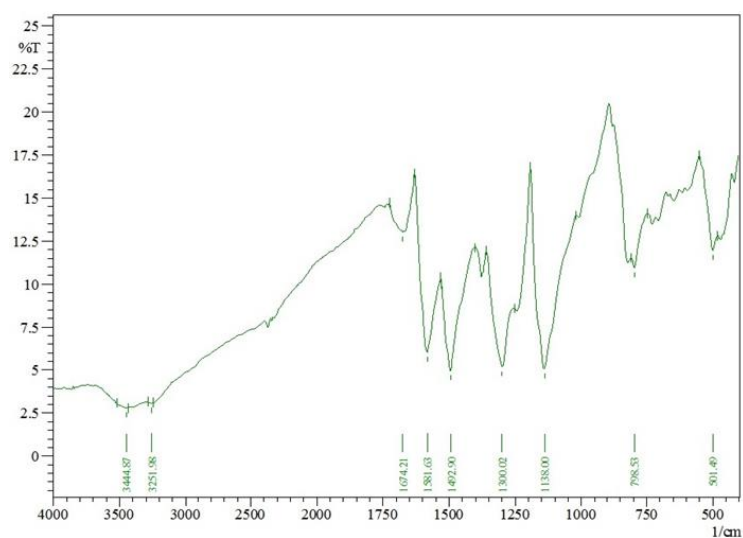


Figure 3. The FT-IR spectrum of GO@PANI-FeF₃.

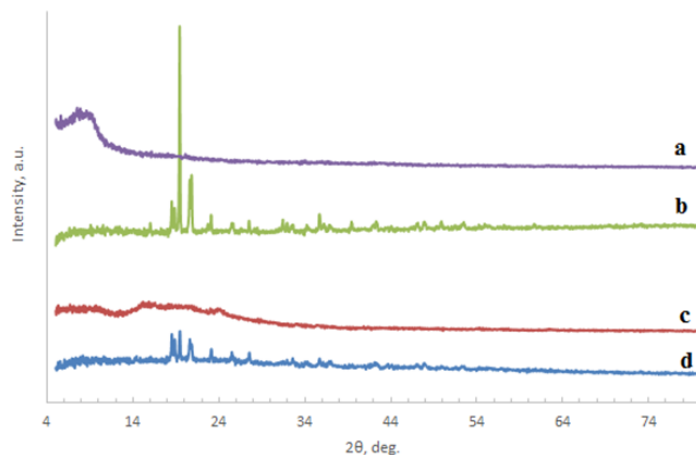


Figure 4. The XRD patterns of GO (a), FeF₃ (b), GO@PANI (c), and GO@PANI-FeF₃ (d).

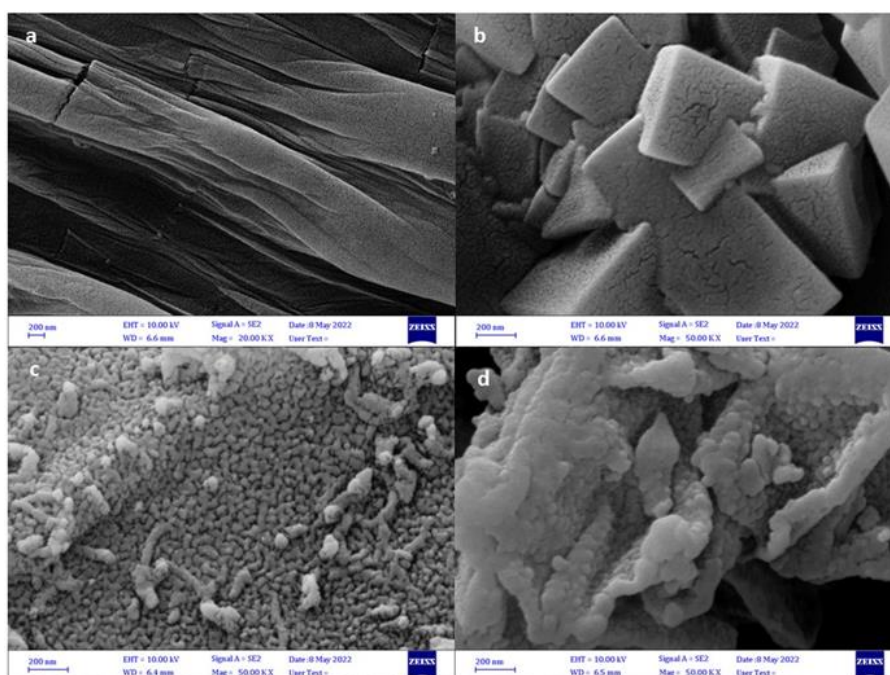


Figure 5. The FE-SEM images of GO (a), FeF₃ (b), GO@PANI (c), and GO@PANI-FeF₃ (d).

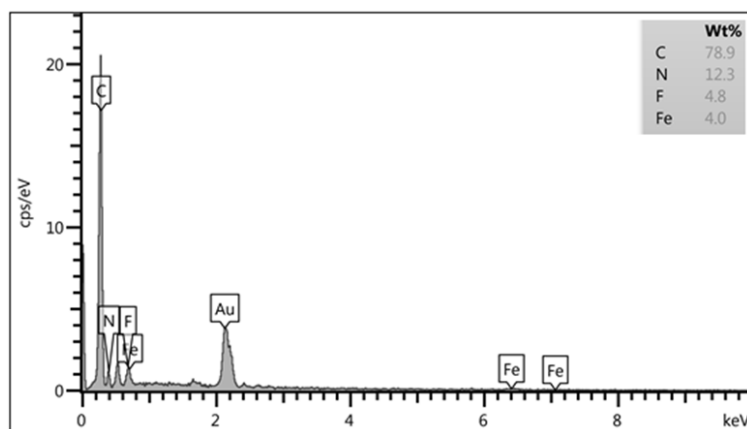


Figure 6. The EDAX analysis of GO@PANI-FeF₃.

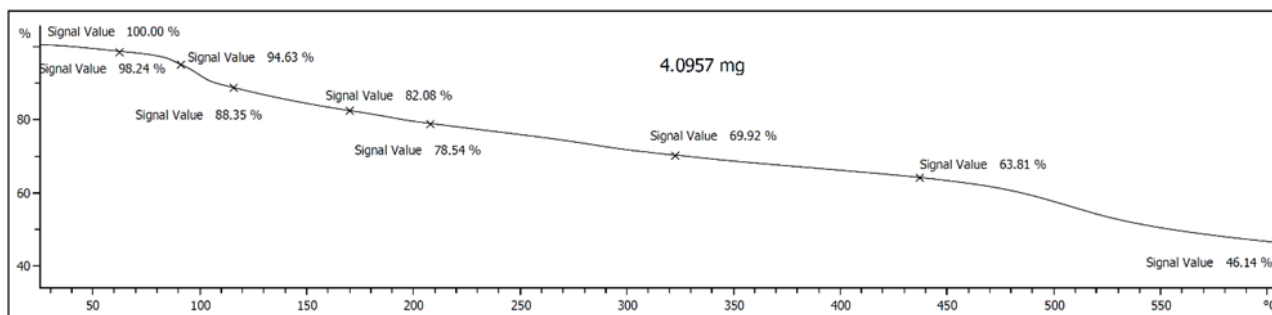


Figure 7. The TG diagram of GO@PANI-FeF₃.

The XRD patterns of GO, FeF₃, GO@PANI, and GO@PANI-FeF₃ are illustrated in Figure 4. The XRD pattern of GO (Figure 4a) showed a broad peak at $2\theta \approx 5.9\text{-}12.9^\circ$ (this is the characteristic peak of GO) [46]. In the XRD pattern of FeF₃ (Figure 4b), some sharp peaks were observed between 8 to 63° [47]. The XRD pattern of GO@PANI (Figure 4c) showed some broad peaks between 5 to 34° , which are ascribed to the structure of GO and polyaniline. By comparing the XRD patterns of GO, FeF₃, and GO@PANI with the pattern of GO@PANI-FeF₃ (Figure 4d), existing GO, polyaniline, and FeF₃ in the structure of final nanocomposite was verified. The FE-SEM images of GO, FeF₃, GO@PANI, and GO@PANI-FeF₃ are represented in Figure 5. As Figures 5a indicates, graphene oxide is formed from sheets with different diameters. According to Figure 5b, the crystals of FeF₃ are as rectangular cuboid with diverse sizes. The FE-SEM image of GO@PANI (Figure 5c) showed covering GO sheets by polyaniline. In the FE-SEM image of GO@PANI-FeF₃ (Figure 5d), covering GO sheets by polyaniline and FeF₃, and formation of thick sheets were observed. The EDAX spectrum of GO@PANI-FeF₃ is exhibited in Figure 6. Surface elemental analysis of the nanocomposite was conducted for C, N, F, and Fe. In the spectrum, the peaks related to the elements and their percentages are shown. The EDAX results confirmed presence of graphene oxide, polyaniline, and FeF₃ in the catalyst structure. TG analysis of GO@PANI-FeF₃ was conducted under

argon atmosphere; the obtained diagram is illustrated in Figure 7.

Addressing the TG diagram, three main weight losses can be observed. The first weight loss (up to $\sim 105^\circ\text{C}$) can be related to evaporation of adsorbed water and volatile solvents on the nanocomposite surface. The second and third weight losses (at $105\text{-}450^\circ\text{C}$ and $450\text{-}600^\circ\text{C}$) can be attributed to the desorption of high molecular weight species, FeF₃ and functional groups, and the destruction of polyaniline and GO structure [48].

The construction of 4H-pyrimido[2,1-b]benzothiazoles using GO@PANI-FeF₃

In order to examine catalytic performance of GO@PANI-FeF₃ in organic reactions, the construction of 4H-pyrimido[2,1-b]benzothiazoles from aryl aldehydes, ethyl acetoacetate and 2-aminobenzothiazole was chosen. Optimization of the reaction conditions was conducted on the construction of 4H-pyrimido[2,1-b]benzothiazole **4c** (Scheme 2); for this purpose, the influence of three variables, including solvent, temperature and amount of GO@PANI-FeF₃, on the reaction was investigated. On basis of the attained data (Table 1), the optimum catalyst amount and temperature were 0.02 g and 90°C , respectively. Moreover, solvent-free conditions were more effectual (entry 10). The reaction was also tested in the absence of catalyst at 110°C in which compound **4c** was obtained in 19% after 250 min (entry 6).

Furthermore, the reaction was examined using GO, GO@PANI and FeF₃ as catalysts; GO and GO@PANI gave the product in 46 and 51%, respectively (entries 13 and 14). FeF₃ afforded 4*H*-pyrimido[2,1-*b*]benzothiazole **4c** in 89% (entry 15); this result was obtained using 0.02 g of FeF₃, but the amount of FeF₃ in 0.02 g of GO@PANI-FeF₃ (optimal conditions) is far fewer than the amount of FeF₃ used in entry 15. Thus, our idea to design graphene oxide@polyaniline-FeF₃ was logical. The scope and limitations of our

protocol for the construction of 4*H*-pyrimido[2,1-*b*]benzothiazoles were investigated thru usage of diverse aryl aldehydes in the reaction; the results are listed in Table 2.

As presented in Table 2, all products were fabricated in high yields and relatively short times; this subject confirmed wide scope of our protocol. Nevertheless, aldehydes bearing electron-withdrawing and halogen substituents gave higher yields in comparison with aldehydes having electron-releasing substituents.

Table 1. Optimization of conditions for the construction of 4*H*-pyrimido[2,1-*b*]benzothiazole **4c**

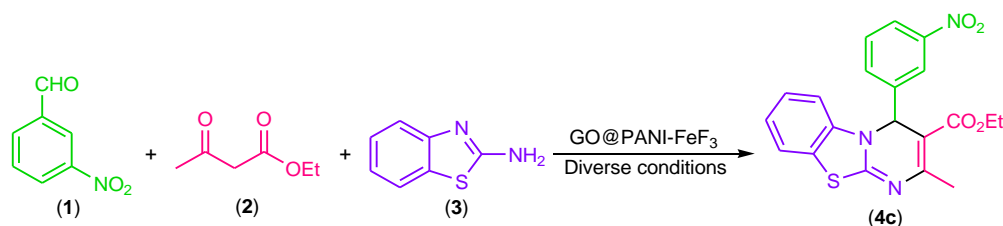
Entry	Solvent	Catalyst amount (g)	Temp. (°C)	Time (min)	Yield (%) ^a
1	EtOH	0.03	Reflux	120	39
2	H ₂ O	0.03	Reflux	120	41
3	Ethylene glycol	0.03	100	120	48
4	THF	0.03	Reflux	120	31
5	CH ₃ CN	0.03	Reflux	120	38
6	Solvent-free	Catalyst-free	110	250	19
7	Solvent-free	0.01	100	120	76
8	Solvent-free	0.01	110	120	85
9	Solvent-free	0.02	100	60	95
10	Solvent-free	0.02	90	60	94
11	Solvent-free	0.02	80	70	86
12	Solvent-free	0.03	80	60	89
13	Solvent-free	0.02 ^b	90	60	46
14	Solvent-free	0.02 ^c	90	60	51
15	Solvent-free	0.02 ^d	90	60	89

^a Isolated yield.

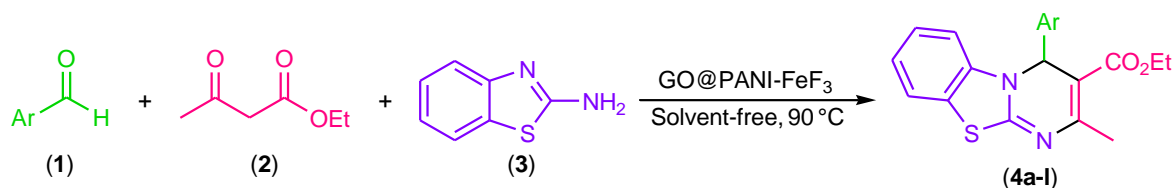
^b GO was used as catalyst.

^c GO@PANI was utilized as catalyst.

^d FeF₃ was applied as catalyst.



Scheme 2. The construction of 4*H*-pyrimido[2,1-*b*]benzothiazole **4c**.

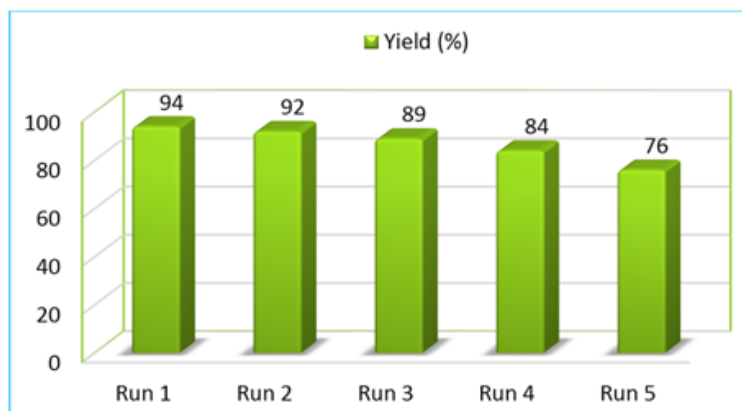
Table 2. The fabrication of 4*H*-pyrimido[2,1-*b*]benzothiazoles using GO@PANI-FeF₃

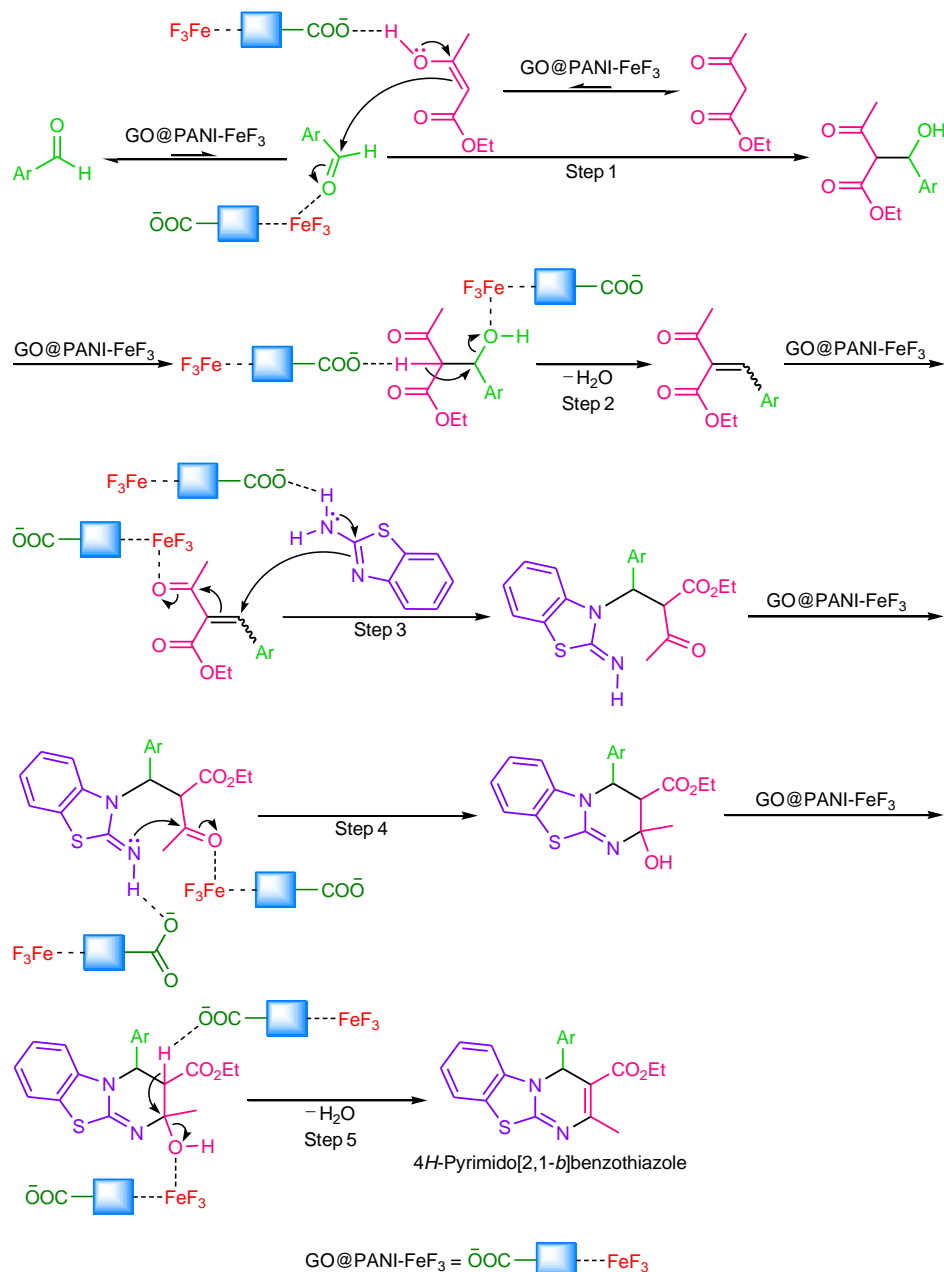
Product	Ar	Time/min	Yield ^a (%)	MP/ ^o C	
				Found	Reported
4a	C ₆ H ₅	70	90	177-179	178-180 [33]
4b	2-O ₂ NC ₆ H ₄	60	91	120-122	122-125 [32]
4c	3-O ₂ NC ₆ H ₄	60	94	224-226	222-224 [33]
4d	4-O ₂ NC ₆ H ₄	60	94	170-172	172-173 [33]
4e	4-HOC ₆ H ₄	70	88	207-209	210-212 [31]
4f	4-MeOC ₆ H ₄	80	86	139-141	140-143 [34]
4g	2-ClC ₆ H ₄	60	90	127-129	124-126 [32]
4h	2,4-Cl ₂ C ₆ H ₃	60	92	132-134	133-135 [32]
4i	4-BrC ₆ H ₄	60	94	113-115	111-113 [33]

^a Isolated yield

To examine the recoverability of GO@PANI-FeF₃, the fabrication of 4*H*-pyrimido[2,1-*b*]benzothiazole **4c** was selected; **Figure 8** illustrates the reusability results. The nanocomposite was reusable for two times with negligible decrement of the yield (runs 2 and 3). However, in third reusing, the yield slightly decreased (run 4). In fourth reusing (run 5), the yield greatly decreased. The reactions time was 60 min.

Scheme 3 depicts the reaction mechanism, which was proposed on basis of the literature [29,31]. GO@PANI-FeF₃ acts as a dual-functional catalyst; FeF₃ is a Lewis acid, and carboxylate anion is a weak base. FeF₃ and carboxylate activate the electrophiles and the nucleophiles, respectively, and facilitate steps 1, 3, and 4. Both species can accelerate tautomerization of ethyl acetoacetate in step 1, and also help removal of H₂O in steps 2 and 5.

**Figure 8.** The reusability results of GO@PANI-FeF₃



Scheme 3. The mechanism

Conclusion


To sum up, we have reported fabrication and characterization of a novel nanocomposite, namely graphene oxide@polyaniline- FeF_3 . Afterwards, we have utilized the nanocomposite as catalyst for the construction of 4H-pyrimido[2,1-*b*]benzothiazoles. Thermal and chemical sustainability of the catalyst, efficiency, relatively short times, high yields of the products,

performing the reaction in solvent-free conditions, reusability of the catalyst, easy work-up, and effortless purification of the products are the advantages of our protocol.

Acknowledgements

The authors acknowledge Research Council of Payame Noor University for the support of this work.

Orcid

Mohammad Kamali-Ardakani : [0009-0004-8511-3027](https://orcid.org/0009-0004-8511-3027)

Esmael Rostami : [0000-0002-6512-9951](https://orcid.org/0000-0002-6512-9951)

Abdolkarim Zare : [0000-0002-8210-3155](https://orcid.org/0000-0002-8210-3155)

References

- [1] I.T. Horváth, *Chem. Rev.*, **2018**, *118*, 369-371. [[Crossref](#)], [[Google Scholar](#)], [[Publisher](#)]
- [2] L.J. Juturi, R. Palavalasa, S.H. Dhoria, S. Jampani, V. Miditana, G. Jalem, *Chem. Methodol.*, **2023**, *7*, 569-580. [[Crossref](#)], [[Publisher](#)]
- [3] Z.Z. Almarbd, N.M. Abbass, *Chem. Methodol.*, **2022**, *6*, 940-952. [[Crossref](#)], [[Publisher](#)]
- [4] M.A. Shahoodh, F.T. Ibrahim, S. Guermazi, *Chem. Methodol.*, **2023**, *7*, 994-1010. [[Crossref](#)], [[Publisher](#)]
- [5] R. Khazaei, A. Khazaei, M. Nasrollahzadeh, *J. Appl. Organomet. Chem.*, **2023**, *3*, 123-133. [[Crossref](#)], [[Publisher](#)]
- [6] F. Hakimi, M. Taghvaei, E. Golrasan, *Adv. J. Chem. A*, **2023**, *6*, 188-197. [[Crossref](#)], [[Google Scholar](#)], [[Publisher](#)]
- [7] M. Farajpour, S.M. Vahdat, S.M. Baghbanian, M. Hatami, *Chem. Methodol.*, **2023**, *7*, 540-551. [[Crossref](#)], [[Google Scholar](#)], [[Publisher](#)]
- [8] Z. Hoseini, A. Davoodnia, M. Pordel, *Adv. J. Chem. A*, **2021**, *4*, 68-77. [[Crossref](#)], [[Google Scholar](#)], [[Publisher](#)]
- [9] F. Esmailzadeh, F. Hassanzadeh-Afruzi, H. Dogari, A. Maleki, *Mater. Sci. Eng. B*, **2023**, *292*, 116420. [[Crossref](#)], [[Google Scholar](#)], [[Publisher](#)]
- [10] W. Yu, L. Sisi, Y. Haiyan, L. Jie, *RSC Adv.*, **2020**, *10*, 15328-15345. [[Crossref](#)], [[Google Scholar](#)], [[Publisher](#)]
- [11] E. Rostami, M.S. Ghorayshi Nejad, *Cellulose Chem. Technol.*, **2021**, *55*, 1095-1108. [[Crossref](#)], [[Google Scholar](#)]
- [12] Z. Atashrouz, E. Rostami, A. Zare, *Res. Chem. Intermed.*, **2022**, *48*, 179-201. [[Crossref](#)], [[Google Scholar](#)], [[Publisher](#)]
- [13] J.B. Zimmerman, P.T. Anastas, H.C. Erythropel, W. Leitner, *Science*, **2020**, *367*, 397-400. [[Crossref](#)], [[Google Scholar](#)], [[Publisher](#)]
- [14] P. Anastas, N. Eghbali, *Green chemistry: principles and practice. Chem. Soc. Rev.*, **2010**, *39*, 301-312. [[Crossref](#)], [[Google Scholar](#)], [[Publisher](#)]
- [15] B. Baghernejad, N. Sharifi Soltani, *Asian J. Green Chem.*, **2022**, *6*, 166-174. [[Crossref](#)], [[Publisher](#)]
- [16] A. Ghanbarpour, A. Khazaei, A.R. Moosavi-Zare, T. Akbarpour, M. Mohammadi, N. Sarmasti, *Polycycl. Arom. Compd.*, **2023**, *43*, 3192-3215. [[Crossref](#)], [[Google Scholar](#)], [[Publisher](#)]
- [17] Z.A.K. Al-Messri, *Chem. Methodol.*, **2023**, *7*, 581-593. [[Crossref](#)], [[Publisher](#)]
- [18] H. Ghafuri, M. Zargari, A. Emami, *Asian J. Green Chem.*, **2023**, *7*, 54-69. [[Crossref](#)], [[Google Scholar](#)], [[Publisher](#)]
- [19] M.T. Gabr, N.S. El-Gohary, E.R. El-Bendary, M.M. El-Kerdawy, *Eur. J. Med. Chem.*, **2014**, *85*, 576-592. [[Crossref](#)], [[Google Scholar](#)], [[Publisher](#)]
- [20] M.K. Singh, R. Tilak, G. Nath, S.K. Awasthi, A. Agarwal, *Eur. J. Med. Chem.*, **2013**, *63*, 635-644. [[Crossref](#)], [[Google Scholar](#)], [[Publisher](#)]
- [21] N. Karalı, Ö. Güzel, N. Özsoy, S. Özbey, A. Salman, *Eur. J. Med. Chem.*, **2010**, *45*, 1068-1077. [[Crossref](#)], [[Google Scholar](#)], [[Publisher](#)]
- [22] C. Kharbanda, M.S. Alam, H. Hamid, K. Javed, S. Bano, Y. Ali, A. Dhulap, P. Alam, M. A.Q. Pasha, *New J. Chem.*, **2016**, *40*, 6777-6786. [[Crossref](#)], [[Google Scholar](#)], [[Publisher](#)]
- [23] P.C. Sharma, K.K. Bansal, A. Deep, M. Pathak, *Curr. Top. Med. Chem.*, **2017**, *17*, 208-237. [[Google Scholar](#)], [[Publisher](#)]
- [24] N. Siddiqui, A. Rana, S.A. Khan, M.A. Bhat, S.E. Haque, *Bioorg. Med. Chem. Lett.*, **2007**, *17*,

- 2007, 4178-4182. [Crossref], [Google Scholar], [Publisher]
- [25] M. Gjorgjieva, T. Tomašič, D. Kikelj, L.P. Mašič, *Curr. Med. Chem.*, **2018**, *25*, 5218-5236. [Crossref], [Google Scholar], [Publisher]
- [26] R. Yadav, D. Meena, K. Singh, R. Tyagi, Y. Yadav, R. Sagar, *RSC Adv.*, **2023**, *13*, 21890-21925. [Crossref], [Google Scholar], [Publisher]
- [27] Y. Yu, W.F. Lu, Z.J. Yang, N. Wang, X.Q. Yu, *Bioorg. Chem.*, **2021**, *107*, 104534. [Crossref], [Google Scholar], [Publisher]
- [28] S. Handique, P. Sharma, *Results Chem.*, **2023**, *5*, 100781. [Crossref], [Google Scholar], [Publisher]
- [29] S. Azad, B.B.F. Mirjalili, *RSC Adv.*, **2016**, *6*, 96928-96934. [Crossref], [Google Scholar], [Publisher]
- [30] M. Kour, S. Paul, J.H. Clark, V.K. Gupta, R. Kant, *J. Mol. Catal. A: Chem.*, **2016**, *411*, 299-310. [Crossref], [Google Scholar], [Publisher]
- [31] B.B.F. Mirjalili, F. Aref, *Res. Chem. Intermed.*, **2018**, *44*, 4519-4531. [Crossref], [Google Scholar], [Publisher]
- [32] A. Dehghani Tafti, B.B.F. Mirjalili, N. Salehi, A. Bamoniri, *J. Iran. Chem. Soc.*, **2022**, *19*, 4377-4388. [Crossref], [Google Scholar], [Publisher]
- [33] B.B.F. Mirjalili, R. Soltani, *RSC Adv.*, **2019**, *9*, 18720-18727. [Crossref], [Google Scholar], [Publisher]
- [34] A. Shaabani, A. Rahmati, S. Naderi, *Bioorg. Med. Chem. Lett.*, **2005**, *15*, 5553-5557. [Crossref], [Google Scholar], [Publisher]
- [35] N. Alishahi, M. Nasr-Esfahani, I. Mohammadpoor-Baltork, S. Tangestaninejad, V. Mirkhani, M. Moghadam, *Appl. Organomet. Chem.*, **2020**, *34*, e5681. [Crossref], [Google Scholar], [Publisher]
- [36] J. Chen, B. Yao, C. Li, G. Shi, *Carbon*, **2013**, *64*, 225-229. [Crossref], [Google Scholar], [Publisher]
- [37] S.J. Tang, A.T. Wang, S.Y. Lin, K.Y. Huang, C.C. Yang, J.M. Yeh, K.C. Chiu, *Polym. J.*, **2011**, *43*, 667-675. [Crossref], [Google Scholar], [Publisher]
- [38] C. Zhang, L. Yao, Z. Yang, E.S.W. Kong, X. Zhu, Y. Zhang, *ACS Appl. Nano Mater.*, **2019**, *2*, 3916-3924. [Crossref], [Google Scholar], [Publisher]
- [39] A. Nekahi, S.P.H. Marashi, D.H. Fatmesari, *Bull. Mater. Sci.*, **2015**, *38*, 1717-1722. [Crossref], [Google Scholar], [Publisher]
- [40] M.E. Uddin, R.K. Layek, H.Y. Kim, N.H. Kim, D. Hui, J.H. Lee, *Compos. B Eng.*, **2016**, *90*, 223-231. [Crossref], [Google Scholar], [Publisher]
- [41] A.M. Das, M.P. Hazarika, M. Goswami, A. Yadav, P. Khound, *Carbohydr. Polym.*, **2016**, *141*, 20-27. [Crossref], [Google Scholar], [Publisher]
- [42] D. Varrica, E. Tamburo, M. Vultaggio, I.D. Carlo, *Int. J. Environ. Res. Public Health*, **2019**, *16*, 2507. [Crossref], [Google Scholar], [Publisher]
- [43] H.V. Hoang, R. Holze, *Chem. Mater.*, **2006**, *18*, 1976-1980. [Crossref], [Google Scholar], [Publisher]
- [44] Q. Xiao, Q. Tong, L.T. Lim, *Food Chem.*, **2014**, *150*, 267-273. [Crossref], [Google Scholar], [Publisher]
- [45] J. Vela, J.M. Smith, Y. Yu, N.A. Ketterer, C.J. Flaschenriem, R.J. Lachicotte, P.L. Holland, *J. Am. Chem. Soc.*, **2005**, *127*, 7857-7870. [Crossref], [Google Scholar], [Publisher]
- [46] L. Stobinski, B. Lesiak, A. Malolepszy, M. Mazurkiewicz, B. Mierzwa, J. Zemek, P. Jiricek, I. Bieloshapka, *J. Electron Spectrosc. Relat. Phenom.*, **2014**, *195*, 145-154. [Crossref], [Google Scholar], [Publisher]
- [47] R. Ma, M. Wang, P. Tao, Y. Wang, C. Cao, G. Shan, S. Yang, L. Xi, J.C. Chung, Z. Lu, *J. Mater. Chem. A*, **2013**, *1*, 15060-15067. [Crossref], [Google Scholar], [Publisher]
- [48] R.A.M. Kunju, J. Gopalakrishnan, *Polym. Eng. Sci.*, **2021**, *61*, 1755-1772. [Crossref], [Google Scholar], [Publisher]

HOW TO CITE THIS ARTICLE

Mohammad Kamali-Ardakani, Esmael Rostami*, Abdolkarim Zare. Graphene Oxide@Polyaniline-FeF₃ (GO@PANI-FeF₃) as a Novel and Effectual Catalyst for the Construction of 4*H*-Pyrimido [2, 1-*b*] Benzothiazoles. *Adv. J. Chem. A*, 2024, 7(3), 236-247.

247

DOI: [10.48309/ajca.2024.428749.1460](https://doi.org/10.48309/ajca.2024.428749.1460)

URL: <https://www.ajchem-a.com/article/187505.html>